Chemical Engineering Journal 170 (2011) 482–491

Contents lists available at ScienceDirect

Chemical Engineering Journal

journal homepage: www.elsevier.com/locate/cej

Enhanced transport of polyelectrolyte stabilized nanoscale zero-valent iron (nZVI) in porous media

Pijit Jiemvarangkul[a], Wei-xian Zhang[b], Hsing-Lung Lien[c,*]

[a] Department of Civil and Environmental Engineering, Lehigh University, Bethlehem, PA 18015, United States
[b] Tongji University, State Key Laboratory of Pollution Control and Resources Reuse, 1239 Siping Rd, Shanghai, China
[c] Department of Civil and Environmental Engineering, National University of Kaohsiung, 811 Kaohsiung, Taiwan

ARTICLE INFO

Article history:
Received 27 October 2010
Received in revised form 24 February 2011
Accepted 25 February 2011

Keywords:
Nanoparticles
Zero-valent iron
Polyelectrolyte
Stabilization
Transport
Groundwater

ABSTRACT

Laboratory experiments including column and batch sedimentation studies were conducted to investigate the transport of nanoscale zero-valent iron (nZVI) particles stabilized by three polyelectrolytes: polyvinyl alcohol-co-vinyl acetate-co-itaconic acid (PV3A), poly(acrylic acid) (PAA) and soy proteins. Results of the continuous packed column study suggest that the both PV3A and PAA can increase nZVI mobility by reducing particle size and generating negatively charged surfaces of nZVI. PV3A stabilized nZVI has the best transport performance among the three materials. It was found that approximately 100% of nZVI flowed through the column. Retardation of nZVI is observed in all tests. Due to the large surface area of nZVI, large amounts of polyelectrolytes are often needed. For example, soy proteins exhibited an excellent stabilization capability only at the dose over 30% of nZVI mass. Approximately 57% of nZVI remained in the column when nZVI was stabilized with PAA at the dosage of 50%. Results suggest that nZVI may be prepared with tunable travel distance to form an iron reactive zone for the in situ remediation.

1. Introduction

Nanoscale zero-valent iron particles (nZVI) have been studied since mid-1990s and have increasingly been applied for environmental remediation and hazardous waste treatment have been studied since 2000 [1–3]. The colloidal iron nanoparticles have large surface areas for rapid uptake and transformation of a large number of environmental contaminants. Reactions of nZVI with chlorinated aliphatic compounds containing either one or two carbon atoms have quickly become classical research literature. Numerous studies have found that nZVI can effectively degrade chlorinated solvents, organochlorine pesticides, PCBs, organic dyes, and inorganic pollutants such as perchlorate, nitrate, and heavy metal ions [4–12].

In addition to its large surface area that provides abundant sites for surface reactions, a proved advantage of nZVI is the simple implementation for subsurface injection and potential for subsurface transport, which enables nZVI to clean up large area of contamination. In this manner, the time, cost and engineering problems associated with constructing conventional iron walls (permeable reactive barriers) can be minimized. Dozens of in situ applications have been reported so far [13–17]. For successful subsurface injection, a stable suspension of nZVI in water is needed. That is, aggregation and sedimentation should be controlled so that transport of nZVI in groundwater can be maintained by Brownian diffusion and advection. Unfortunately, owing to the relatively high ionic strength of groundwater favorable for colloidal aggregation and the high density of iron, bare nZVI without proper surface modification has very limited mobility in the subsurface. Laboratory studies have shown that nZVI typically exists as micron sized aggregates in water [18–20].

Dispersion of nZVI is more a skill of art than science at present time. It is likely that some of the most important factors affecting the aggregation and transport of nZVI are still to be identified. For example, the effects of magnetic forces and high solution pH on nZVI aggregation and filtration have not been examined. Based upon theories of colloidal aggregation in water, it has been generally assumed that nZVI suspension in water depends on the net effect of attractive and repulsive forces among nZVI particles. According to the DLVO theory, the overall stability of a colloidal system is determined by the sum of van der Waals attraction and electrostatic double layer repulsion [21]. The DLVO theory predicts that an energy barrier exists, which prevents the aggregation of some colloidal particles. Compared to micro sized colloids, evidence suggests that nanoparticles have stronger tendency to aggregation/coagulation. This has been attributed to smaller particle size and reduced surface potential.

* Corresponding author.
E-mail address: lien.sam@nuk.edu.tw (H.-L. Lien).

1385-8947/$ – see front matter © 2011 Elsevier B.V. All rights reserved.
doi:10.1016/j.cej.2011.02.065

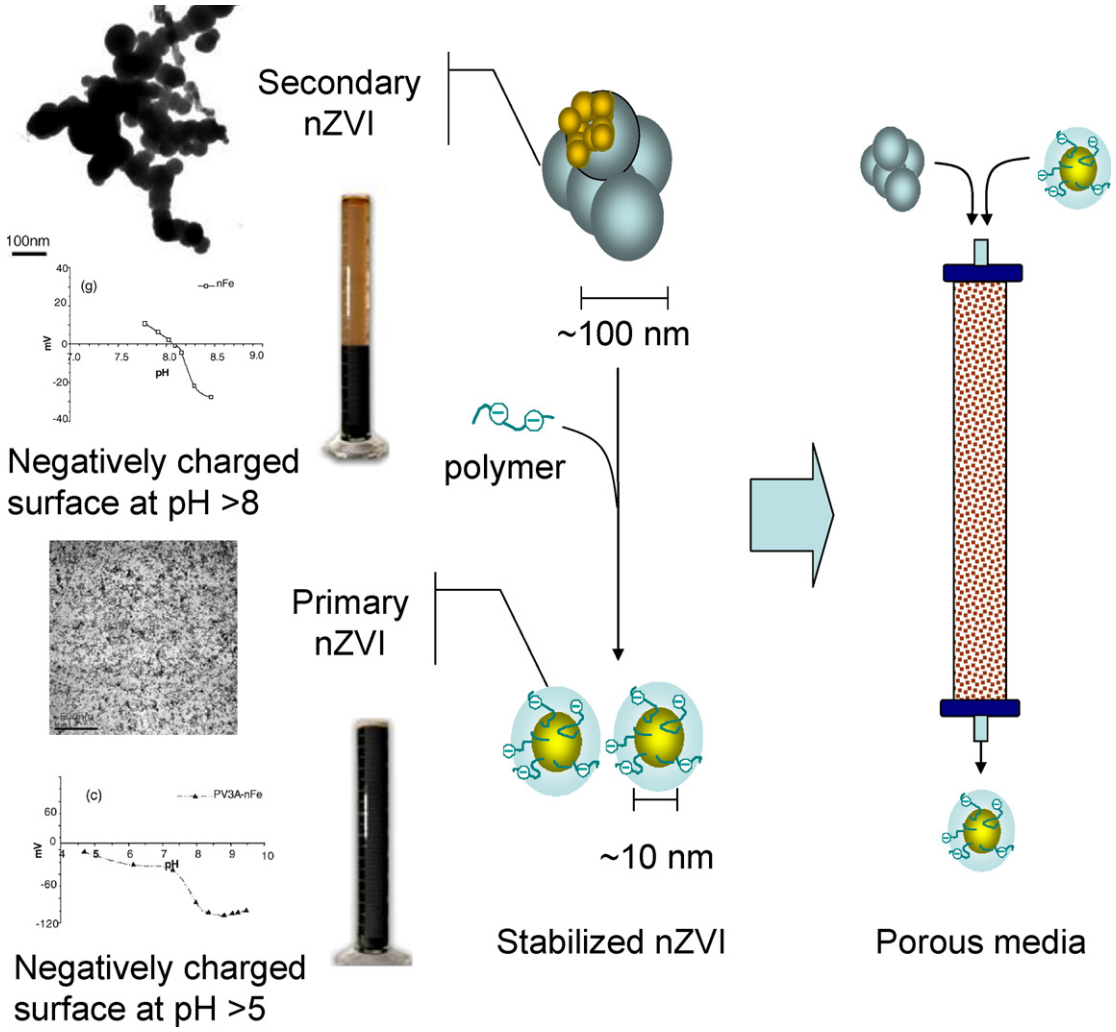

Fig. 1. Concepts of nZVI stability and transportability.

To create and maintain stable suspension of nZVI particles, a common strategy is to increase the repulsive electrostatic forces. Several studies have reported that the certain polymeric materials are able to stabilize nZVI in water. A wide array of polymers has been investigated including poly acrylic acid (PAA), polyvinyl alcohol-co-vinyl acetate-co-itaconic acid (PV3A), polyaspartate (PAP), Tween 20 and biopolymer such as soy proteins, starch, and carboxymethyl cellulose (CMC) [22–28]. Among them, PAA is the first polymer used to disperse nZVI for the field remediation while CMC has recently been tested in the field [15]. In general, the polymers consists of polar anchoring groups (e.g., –COOH, –OH, –C=O) and a stabilizing hydrocarbon chains. The anchoring groups can chemically or physically attach onto the surface of nZVI while the stabilizing chains in water can waggle around and take up varied configurations. Overlap of these flexible chains associated with the neighboring particles produces electrostatic and steric repulsions between particles and can thus stabilize the particles under certain conditions [29]. Our previous work has demonstrated that PV3A provides great electro-steric stabilization for nZVI [18,19]. As illustrated in Fig. 1, in the absence of PV3A, the bare nZVI, has a particle size of about 100 nm that is apparently a loose aggregate of numerous primary ZVI nanoparticles with the size less than 10 nm [19]. The bare nZVI aggregates and precipitates in a few min. With the addition of PV3A, nZVI with the size of about 15 nm can exist in water for months [30]. Not surprisingly, the PV3A stabilized nZVI moves swiftly in laboratory soil columns.

The electro-steric stabilization is a common method that has been used to improve the mobilization of particles in solution by adding ionic polymeric molecules such as polyelectrolytes [31]. The polyelectrolytes containing a net negative or positive charge at near neutral pH not only sterically stabilize particles but also increase surface charges of particles that prevent particles from the aggregation and reduce size of particle clusters. As illustrated in Fig. 1, the surface zeta potential of PV3A stabilized nZVI is negative within a wide range of pH (>5) while the surface of bare nZVI is negatively charged only when pH is greater than 8. Thus, during the particle transport, the electrostatic repulsive force induced by the polyelectrolyte not only stabilizes nanoparticles themselves but also prevents nanoparticles from the precipitation at the surface of porous media, which is negatively charged.

Though extensive studies have been conducted to investigate the nZVI stabilization and transport in porous media, the particle concentrations were relatively low (0.1–6 g/L) [32–35]. The use of low particle concentrations is because nZVI tends to agglomerate at high particle concentrations even in the presence of polymers [34]. However, our field experience suggests that the injection concentration of nZVI should be greater than 8–10 g/L in order to establish an effective remediation in the aquifer. Thus, the objective of this study is to develop a polymer stabilized nZVI that can be used at high injection concentration (10 g/L). We have screened nearly 20 polymers for the stabilization of nZVI in aqueous solution (Table 1). In addition, several biomaterials have also been examined including

Table 1
Commonly used polymers for sterically stabilized aqueous dispersions.

Anchoring groups	Stabilizing chains
Polystyrene	Polyethylene oxide
Polyvinyl acetate	Polyvinyl alcohol
Polymethyl methacrylate	Polyacrylic acid
Polyacrylonitrile	Polymethacrylic acid
Polydimethylsiloxane	Polyacrylamide
Polyvinyl chloride	Polyvinyl pyrrolidone
Polyethylene	Polyethylene imine
Polypropylene	Polyvinyl methyl ether
Polylauryl methacrylate	Poly(4-vinyl pyridine)
Polypropylene oxide	

starch and soy proteins. In this work, results on the effects of PV3A, PAA and soy proteins are presented. Bath sedimentation experiments and continuous packed column studies were conducted to investigate the nZVI stabilization and the transport behavior of the stabilized nZVI particles. To the best of our knowledge, the concentration of polymer stabilized nZVI used in this study to simulate the field conditions is the highest dose applied in column studies so far.

2. Materials and methods

2.1. Materials

ACS grade ferric chloride ($FeCl_3$) was purchased from Alfa Aesar. Sodium borohydride ($NaBH_4$) with 98% purity was obtained from Finnish chemicals (Finland). Polyvinyl alcohol-co-vinyl acetate-co-itaconic acid (PV3A) and sodium bromide (NaBr) were from Aldrich. Poly(acrylic acid), sodium salt (PAA) with molecular weight ranging from 4,300 to 4,400 g/mol and 40 wt% solution was purchased from Polysciences, Inc. Standard Ottawa sand, designated as ASTM 20/30 was from U.S. Silica Company. Hydrochloric acid (12.1 N) and nitric acid (15.8 N) were purchased from EMD Chemicals and Fisher Chemicals, respectively. Soy proteins (Gold 300 soy powder, 300 mesh) with 40% protein and 20% fat were obtained SoyLink^{TM}, Iowa.

2.2. Synthesis of nZVI

nZVI used in this work was prepared with the reduction of ferric chloride by sodium borohydride. Equal volumes of 0.94 M $NaBH_4$ and 0.18 M $FeCl_3$ were quickly mixed in a batch reactor. The borohydride was slowly metered into the ferric chloride solution stirred at ~400 rpm. The redox reaction can be formulated as follows:

$$4Fe^{3+}{}_{(aq)} + 3BH_4{}^{-}{}_{(aq)} + 9H_2O \rightarrow 4Fe^{0}{}_{(s)} + 3H_2BO_3{}^{-}{}_{(aq)} + 12H^{+}{}_{(aq)} + 6H_{2(g)} \quad (1)$$

Additional 10 min were given to complete the reaction after the titration was completed. The formed iron nanoparticles were harvested by vacuum filtration through 0.2 μm filter papers. The iron particles were then washed several times with DI water and ethanol before use. The average particle diameter of nZVI was around 60–70 nm, as determined by scanning electron microscopy and a combined acoustic/electroacoustic spectrometer [19]. Detailed procedures on the nZVI synthesis and characterization have been previously published [18,19]. The finished nanoparticles were washed with ethanol, purged with nitrogen, and refrigerated in a sealed polyethylene container under ethanol (<5%) until use. The residual water content of the nanoparticles as used typically varied between 60 and 70%.

2.3. Synthesis of polymer stabilized nZVI

PV3A, PAA and soy powder were used in this work to prepare aqueous suspensions of nZVI. Fig. 2 illustrates the molecular structure of PV3A, PAA and soy proteins. PV3A, with molecular weights in the range of 4300–4400 is a food grade material, biodegradable and nontoxic, likely due to the presence of highly biodegradable –OH, –CO–, and –COOH groups in the molecules [13]. PAA with molecular formula $[CH_2CH(CO_2Na)]_n$ contains carboxylic acid (–COOH) groups for stabilizing nZVI. In an alkaline solution, carboxylate is assumed to be the anchors coordinating onto the iron surface [36,37] and thus provide iron particles with additional charges. Monomers of natural soy proteins have amino acid residues linked by amide bonds to form polypeptide chains (Fig. 2) [38]. The polypeptide chains can interact with each other and entangle into complicated three-dimensional structures by disulfide and hydrogen bonds with a molecular weight ranging from 300,000 to 600,000 Da. Soy proteins can be divided into water-soluble albumins and salt solution-soluble globulins. Most soy proteins are globulins, containing about 25% acidic amino acids, 20% basic amino acids, and 20% hydrophobic amino acids [38].

PV3A stabilized nZVI was prepared in a 500 mL flask reactor with three open necks. The center neck hosted a mechanical stirrer with a speed set at 60 rpm. 2 g/L of nZVI particles was added with PV3A with the mass ratio of PV3A to nZVI from 0.05 to 0.1. In other words, the dose of PV3A accounted for 5–10% of nZVI mass. The solution was mixed for 2 h at pH 9.5–10 under ambient temperature conditions (23 ± 0.5 °C). Similar procedures were also conducted for synthesizing the PAA and soy proteins stabilized nZVI. During each experiment, suspended solids, suspended iron, solution pH and Eh were measured while nZVI was characterized using transmission electron microscopy (TEM).

Table 2
Parameters of sand columns for nZVI transport experiments.

	Bare-nZVI	PV3A-nZVI	PAA-nZVI
Flow rate (mL/min), Q	10.0	3.0	10.0
Bed volume (mL), BV	58.9	58.9	58.9
Porosity (θ)	0.4	0.4	0.4
Grain size (mm)	0.6–0.85	0.6–0.85	0.6–0.85
Column length (cm), L	30	30	30
Column inner diameter (cm), D_i	2.5	2.5	2.5
Darcy velocity (cm/s), V_d	0.034	0.01	0.034

2.4. Stability test of nZVI

Batch sedimentation experiments were conducted to assess stability of nZVI dispersion. A 200 mL suspension of 10 g/L nZVI and polyelectrolytes were mixed for 2 h. To investigate the polyelectrolyte dose effect, the mass ratio of polyelectrolyte to iron was set in the range of 0–1. The suspension was mixed at a speed of 500 rpm at room temperature. Afterward, the solutions were transferred into 100 mL cylinders to observe the sedimentation of nZVI for 180 min. Before the experiment, iron samples were taken to measure the total iron concentration and pH of each solution. Total solids and iron concentration in solutions after settling were also measured.

2.5. nZVI transport experiment

Fig. 3 illustrates the setup of column experiments. Glass columns with 30 cm in length and 2.5 cm in diameter were packed with sand for the nZVI transport experiments. Standard Ottawa sand, designated as ASTM 20/30 (American Society for Testing and Materials) was used as the column media. The ASTM 20/30 sand is composed of mineral quartz (>99.8%, silicon dioxide, SiO_2). Its color is white, the specific density is 2.65 g/cm^3, and the grain shape is closely rounded. The particle size is in the range of 0.60–0.85 mm. Main parameters of the column experiments are summarized in Table 2. A few glass beads of 3 mm diameter were placed at both ends of the

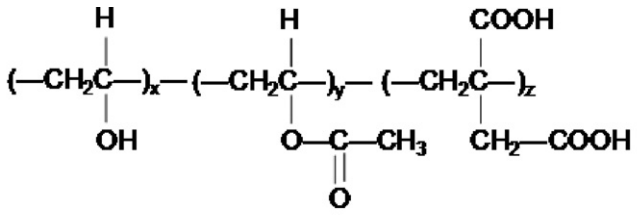

(a) Polyvinyl alcohol-co-vinyl acetate-co-itaconic acid (PV3A)

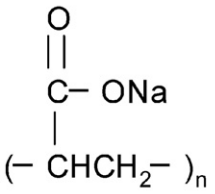

(b) Poly acrylic acid (PAA)

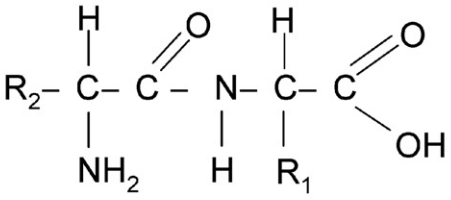

(c) Soy proteins: An example of representative molecular structure

Fig. 2. Molecular structures of (a) polyvinyl alcohol-co-vinyl acetate-co-itaconic acid (PV3A), (b) poly acrylic acid (PAA), and (c) soy proteins.

column to prevent the loss of the sand and facilitate the flow distribution. The column was set up vertically and sealed with screw caps at both ends.

For the transport of PAA stabilized nZVI, a 200 mL solution containing PAA stabilized nZVI was pumped upward through the column as illustrated in Fig. 3. The flow rate was approximately 10 mL/min measured at the effluent port of the column. After completing the injection at 3.4 pore volumes (PV), 700 mL DI water was introduced into the column to flush the remaining particles inside the column. To prevent the nZVI from the sedimentation, the sus-

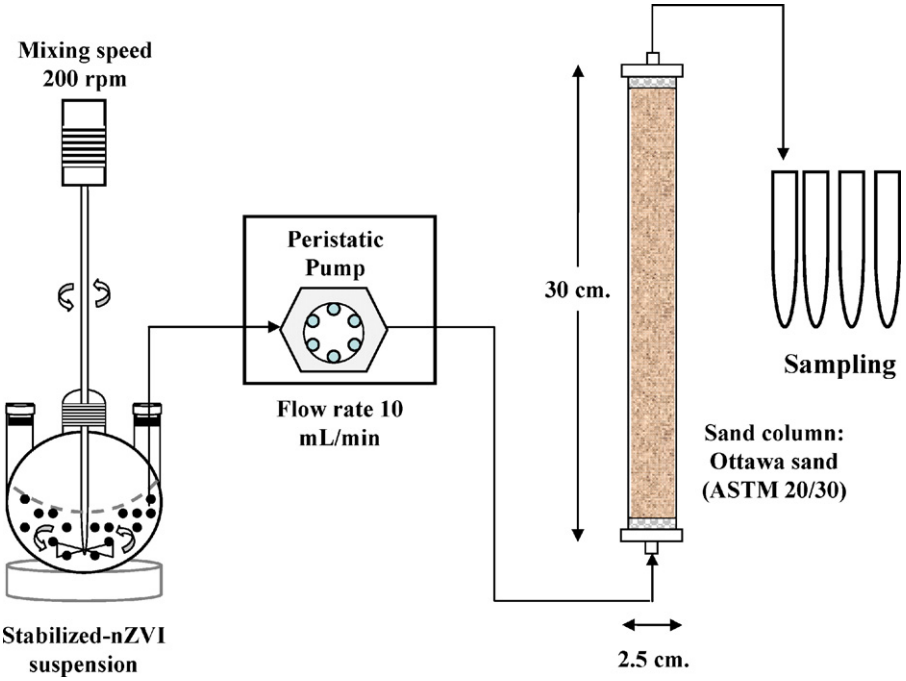

Fig. 3. Schematic of column experiments.

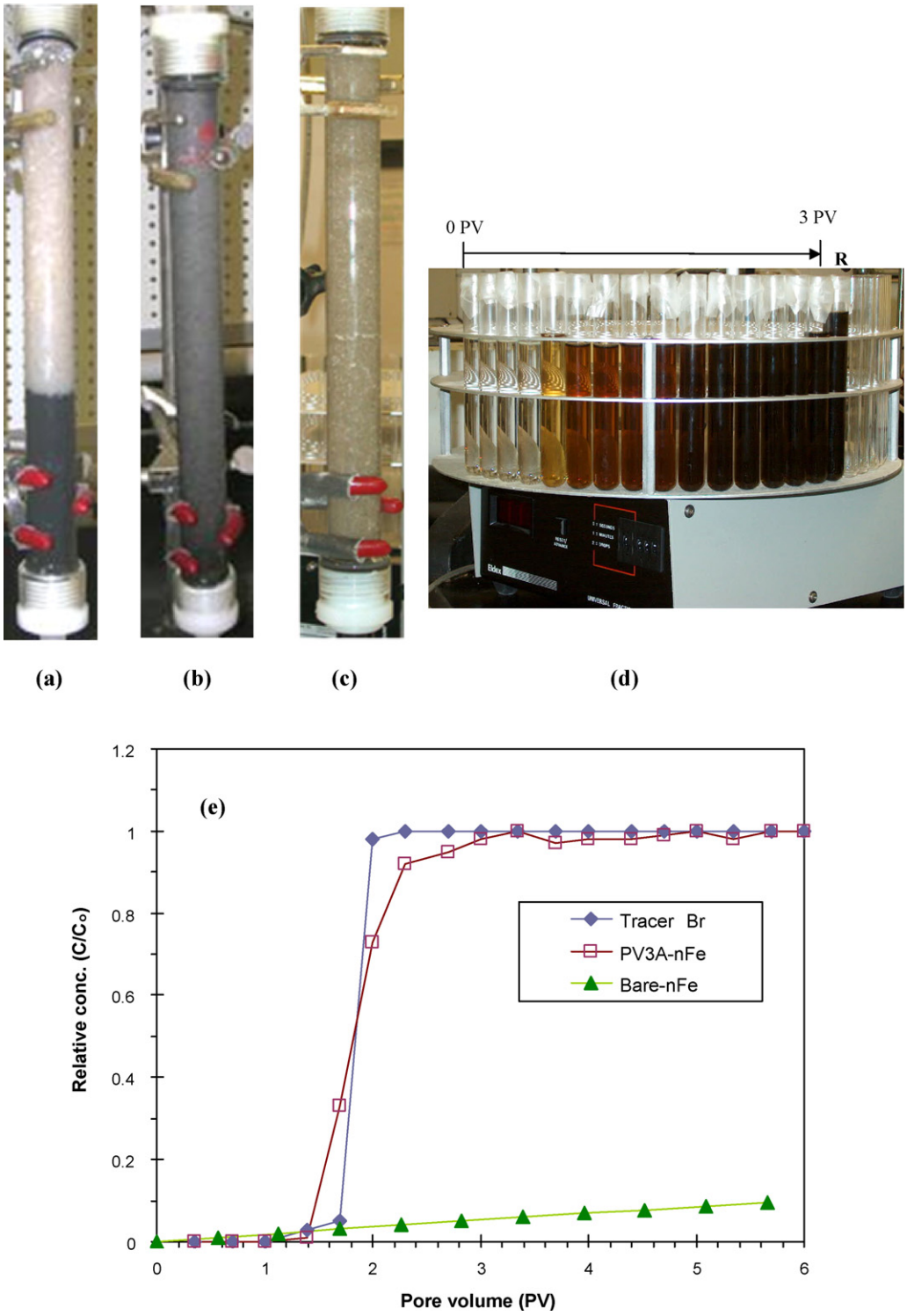

Fig. 4. (a) Photograph of the column after bare nZVI injected; (b) photograph of the column after the complete injection of PV3A stabilized nZVI and (c) flushed by DI water; (d) the collection of the effluent containing PV3A stabilized nZVI (the tube labeled R is the initial stabilized nZVI slurry for comparison) and (e) breakthrough curves of the column experiment for PV3A stabilized nZVI and bare-nZVI.

pension was mixed at 200 rpm. The iron concentration measured in the influent was about 10 g/L. For the transport of PV3A stabilized nZVI, a concentration of 2 g/L of PV3A stabilized nZVI was tested in the experiments. It should be pointed out that the injection concentration of PV3A-stabilized nZVI used in this work follows the concentration of nZVI used in the field work [2]. As shown in Fig. 3, the inflow was connected to the flask reactor where the nZVI was mixed at 200 rpm to maintain the suspension. The flow rate (~3 mL/min) was determined at the effluent port of the column. The effluent stream was collected by a fraction collector at selected time intervals. The solid content and iron concentration of effluent samples were determined. The transport of bare nZVI was also conducted as control tests. The operation conditions were listed in Table 2.

Bromide (Br^-) is commonly used as the non-adsorbing and non-retarded tracer in column experiments [39]. In this work, bro-

mide in the form of sodium bromide (NaBr) was dissolved in DI water with a concentration of 0.5 mM. The tracer was continuously pumped into the column till the effluent concentration is equal to the influent. The effluent bromide was collected at a selected time interval and the concentration was determined by an Ion Chromatography (IC) (ICS-90, Dionex), which was equipped with an analytical column (IonPac® AS4A-SC 4 mm × 250 mm, Dionex) and a detector (Model DS5 Detection Stabilizer, Dionex) for anion analysis. The results were used to determine porosity of the sand column and retardation of nZVI transport.

2.6. Analytical methods

2.6.1. Transmission electron microscopy (TEM)

Images of nZVI were recorded with a Philips EM 400T TEM (Philips Electronics Co., Eindhoven, Netherlands) operated at 100 kV. The TEM samples were prepared by depositing two to three droplets of the sample suspension onto a holey carbon film (Ernest Fullam, Inc., Latham, NY), which was completely dried in a fume hood prior to the TEM analysis.

2.6.2. Total solid concentration

Evaporation method was used to measure the solids content of a solution. 5 mL of nZVI sample was poured into 100 mm diameter-weighing pan and dried at 105 °C for 24 h. Afterward, the weight of the sample pan was measured and the solid concentration was determined.

2.6.3. Total iron concentration

Atomic absorption (AA) method was used to measure the iron concentration in solution samples. 1 mL nZVI suspension was first transferred into a 100 mL volumetric flask and mixed with 50 mL of 2.4 N of HCl and 0.27 N of HNO_3. The solution was mixed for 1 h. DI water was then added to make up the solution to 100 mL. The solution was then diluted for AA analysis. A Perkin Elmer AAnalyst 200 Atomic Absorption Spectrometer was used in this work.

2.6.4. pH/standard potential (E_h) measurement

A combination pH electrode (Orion) was used in conjunction with a Sension1 (Hach) meter to track solution pH. It was calibrated prior to each test. A combination Ag/AgCl reference electrode (Cole-Parmer) was used with a Model 420A pH/ORP meter (Orion) to monitor redox potential and was calibrated with fresh ZoBell solution before each test. Measured redox potential readings (mV) were converted to E_h, the potential relative to the standard hydrogen electrode, as a function of solution temperature by adding +199 mV at 25 °C.

3. Results and discussion

Fig. 4 contains main characteristics of the polyelectrolyte stabilized nZVI in the sand column. Photographs of the columns after the injection of bare nZVI are presented for comparison. For the bare nZVI in the absence of the electrolytes (Fig. 4a), most of nZVI deposited at the bottom section (the entrance end) of the column. No visible black iron can be seen in the effluent end. Fig. 4(b) and (c) are photos of the PV3A stabilized nZVI. Black nZVI quickly moved up in the column, and quickly filled up the entire column. The black color nZVI was clearly visible in the effluent with gradually increasing concentration during the period of 3 pore volumes (PV) injection (Fig. 4d). After the influent was switched to pure water, the PV3A stabilized nZVI can be completely flushed out of the column with about three pore volumes of DI water, suggesting a low sticking probability of the PV3A stabilized nZVI (Fig. 4(c)).

Fig. 4(e) presents the breakthrough curves of column experiments for PV3A stabilized nZVI and bare nZVI. A tracer (bromide)

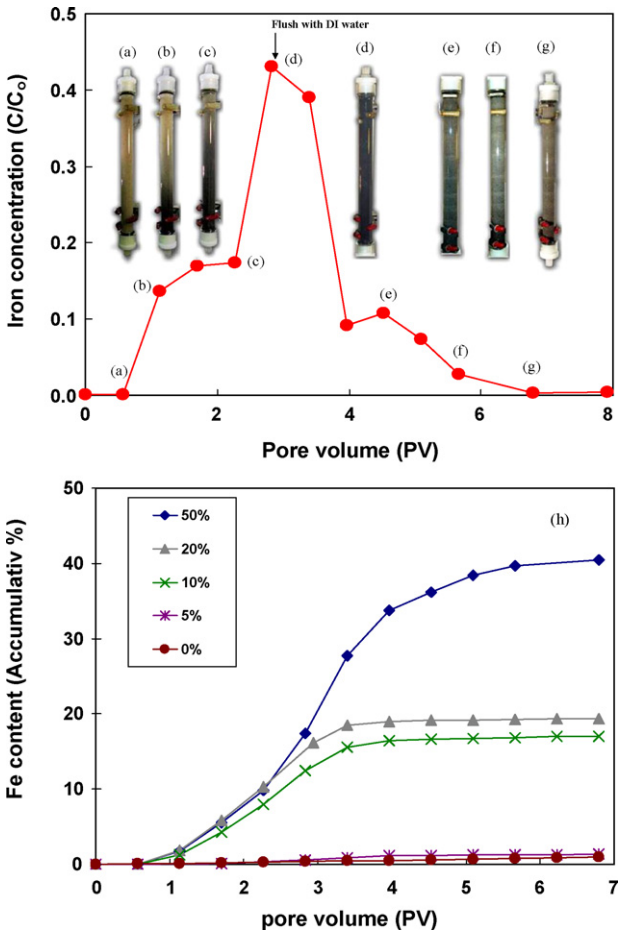

Fig. 5. The breakthrough curve of the column experiment for PAA stabilized nZVI at the PAA dosage of 50%. Photographs of the column labeled from (a) to (g) were taken during the nZVI transport corresponding to the specific sampling time shown in the breakthrough curve. (h) The accumulative curve of iron in the effluent during the course of PAA stabilized nZVI transport in the column. The PAA dosage varies from 0 to 50%.

was used for control and baseline measurements. For the PV3A stabilized nZVI, iron concentration in the effluent reached the same level as that in the influent ($C/C_0 = 1$), suggesting completely breakthrough. The break point at $C/C_0 = 0.95$ is around 2 PV, compared to 1.5 PV of the tracer. This shows that the retardation effect is small for the transport of PV3A stabilized nZVI in the column. In contrast, the relative concentration (C/C_0) in the effluent for the bare-nZVI is no more than 0.15 over 6 PV, suggesting most of the bare nZVI was retained in the column. As confirmed in our previous work, PV3A reduces the size of nZVI and moreover, creates highly negative-charged surfaces [19]. Both the steric repulsion caused by the large PV3A molecules and electrostatic repulsion created by the dissociation of the carboxylic acid groups on the PV3A molecules are likely in play and favor nZVI particles move through the sand column.

The data presented in Fig. 4(e) can be further used to calculate the dimensionless attachment efficiency factor (α) for nZVI transport [40]:

$$\alpha = -\frac{2}{3}\frac{d_c}{(1-\theta)L\eta_o}\ln\left(\frac{C}{C_0}\right) \quad (2)$$

where d_c is the diameter of single spherical collector, θ is the porosity of the medium, L is the filter medium packed length, C/C_0 is the normalized particle concentration obtained from the breakthrough curve, and η_0 is the predicted clean bed single-collector efficiency. Values of various parameters are summarized in Table 2 and η_0 is estimated according to the work of Tufenkji and Elimelech

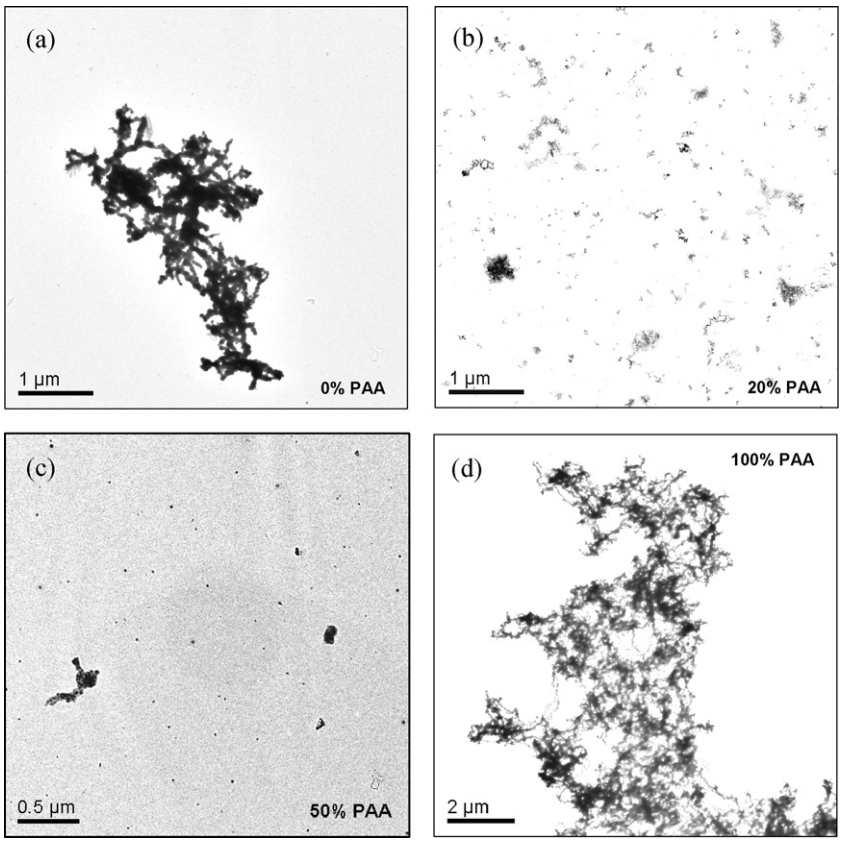

Fig. 6. TEM images of nZVI stabilized with various PAA dosage: (a) 0%, (b) 20% (c) 50% and (d) 100%.

[40]. Hence, the PV3A stabilized nZVI has the attachment efficiency factor of about 4.7×10^{-4} at $C/C_0 = 0.99$. The attachment efficiency factor of 4.7×10^{-4} may match the low-end value of natural colloids (with α typically less than 0.05). In other words, the stabilized nZVI is indeed stable in water compared to naturally occurring colloidal particles.

The transport of PAA stabilized nZVI was also examined with the same column experiments (Fig. 5). Preliminary tests showed that PAA is less effective than PV3A so the PAA to iron ratio was increased to 0.5. Total iron passing through the column was measured as a function of pore volume as shown in Fig. 5. nZVI gradually moved from the bottom to the top of the column. The column color changed from brown to black (Fig. 5(a)–(d)). The highest iron content in the effluent was determined to be 45% of the influent iron level at 2.8 PV. After completing the injection of nZVI at 3.4 PV, DI water was pumped into the column to flush the nZVI deposited in the column. As the particles were washed out, the column gradually turned to brown (Fig. 5(e)–(g)). There was a small peak appearing at 4.5 PV. The split peak may be attributed to some large nZVI that migrated slowly in the column and was flushed out by DI water. In other words, the particles have a range of sizes.

Unlike the PV3A stabilized nZVI, PAA stabilized nZVI exhibited significant retardation effect. Fig. 5(h) depicts the accumulative iron mass in the effluent as a function of influent PV. For the test of bare nZVI, the results show that less than 1% of iron came out from the column over the experiment duration. Similarly, at the low PAA dosage (5%), only a small amount of iron was ever detected in the effluent. Increase in the PAA dosage did increase in the iron transport out of the column. For example, about 18% of the total iron was obtained in the effluent when the PAA dosage increased to 10%. The total iron mass recovered in the effluent accounted for nearly 43% of the initial iron mass when the PAA dosage was increased to 50%. Though Kanel et al. reported PAA-stabilized nZVI (4 g/L) can be transported like a tracer without significant retardation in a two dimensional sand box [41], the retardation was still observed in one dimensional packed sand column at the particle concentration greater than 0.5 g/L [35]. Obviously, PAA and PV3A have different molecular size and charge density, which in turn affect the overall stability of nZVI in water.

Transportability of nanoparticles in the porous media is mainly dependent on the particle size, stability of the suspension and particle charge. Earlier studies on turbidity penetration in the aquifer have indicated that natural colloidal particles particularly those about 1–0.1 μm in diameter can penetrate in the porous media for an appreciable distance [42]. As shown in Fig. 6, bare nZVI without stabilizers aggregates and forms chain-like clusters, though the primary iron nanoparticles may have the size of 1–10 nm in diameter. With the addition of polyelectrolyte stabilizers, a more stable suspension of nZVI can be attained. Fig. 6 also shows the TEM images of nZVI particles stabilized with various dosage of PAA. For the PAA dosage of 20 and 50%, the TEM images show that PAA serves an agent preventing nZVI from the aggregation (Fig. 6(b) and (c)). However, with the PAA dosage at 100%, the chain-like clusters of nZVI were reemerged. The clusters formed at high PAA dose show looser structure than bare nZVI cluster structures. The chain-like clusters that are a consequence of weak attractive forces have been reported in extensive studies of bare nZVI (e.g., [43]). The gel-like network of PAA bridges nZVI particles when excessive amount of PAA is used [44].

Stability of nZVI suspensions was further tested by sedimentation experiments. Without polyelectrolytes, bare nZVI settled in a few min. Fig. 7 shows the total solid concentration of stabilized nZVI solution after settling for 180 min. At the low PAA dosage (<5%), the solutions have low solid content and the upper liquid is clear because most of nZVI was aggregated and settled. The solid content accounted for less than 5% of the total iron mass. The total solid con-

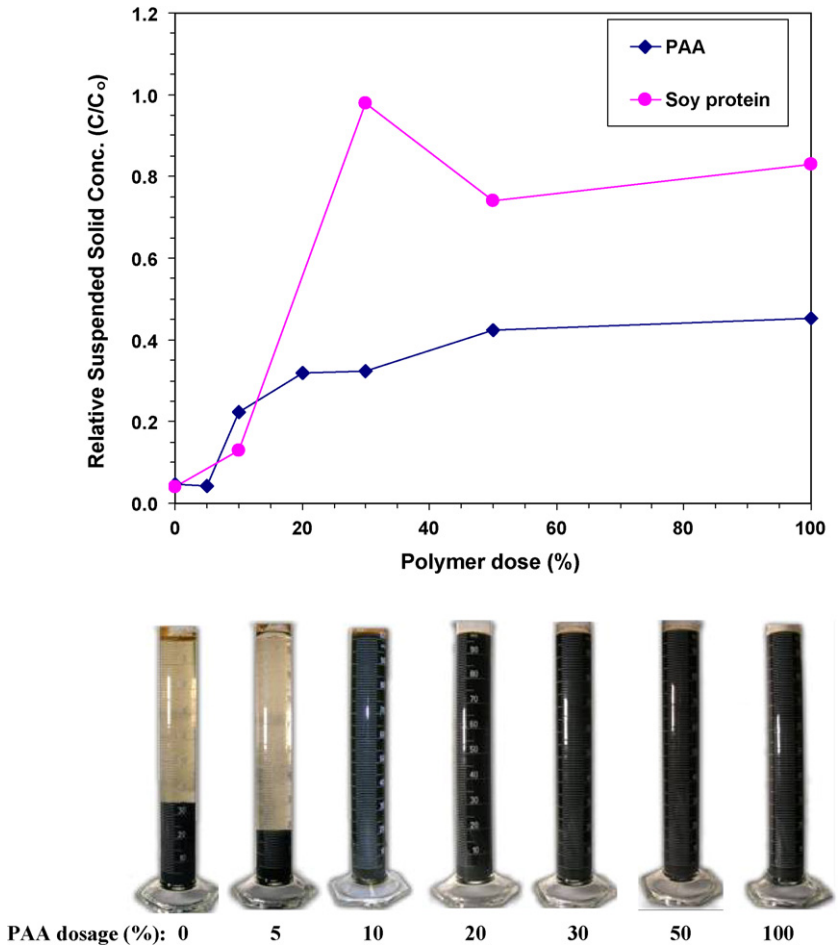

Fig. 7. Effect of the dosage of PAA and soy protein on the dispersion of nZVI after settling for 180 min.

centration and the total iron concentration analyzed by AA are well correlated because the nZVI is the only solid in the system. The solid concentration in solution rapidly increased to 22% at PAA dosage of 10% and continuously increased to 43% at PAA dosage of 50%. A slow increase in the solid content to 45% was observed at the PAA dosage of 100%. It is apparent that the nZVI stability is a function of the PAA dosage. Increase in the PAA dosage resulted in the enhancement of the nZVI stability. However, an excessive amount of PAA was not beneficial to the suspension of nZVI. This is consistent with the TEM analysis shown in Fig. 6. Similar to the PAA, the soy proteins are also capable of stabilizing nZVI in the solution. As depicted in Fig. 7, nearly 100% of nZVI was suspended in the solution at the soy protein dosage at 30%. However, the stability decreased when the soy protein dosage exceeded 30% of the total iron mass, suggesting the overdose undermined nZVI stabilization.

In general, aquifer materials are negatively charged; thus, a negatively charged surface of particles would be favorable for particle transport. The zero-point of charge (pH_{zpc}) has been determined to be 8.1 for bare nZVI [18,19]. In other words, the nZVI surface is negatively charged at pH greater than 8.1. At near neutral pH, bare nZVI has positive charges, which are detrimental to nZVI transport due to the rapid attachment to aquifer materials. On the other hand, both PAA and PV3A stabilized nZVI showed a relatively low value of pH_{zpc}. For example, the addition of PV3A significantly converted nZVI to a negatively charge over a wide pH range. The pH_{zpc} of PV3A stabilized nZVI was measured to be about 4.7. Consequently, the polyelectrolyte stabilized nZVI possesses strong electrostatic repulsion against the attachment to aquifer materials under neutral pH conditions.

In this work, polyelectrolytes such as PV3A and PAA were demonstrated to enhance nZVI mobility and dispersion. PV3A has been used as a dispersant generating nZVI with substantially better subsurface mobility potential [19]. Previous work by Mallouk and coworkers has confirmed that PAA binding to nZVI creating highly negative surfaces effectively reduces the filtration removal by aquifer materials [22]. Based upon this work, the results confirmed that the transport efficiency of nZVI in porous media can be enhanced by the increase of the PAA dosage. Fig. 8 shows the

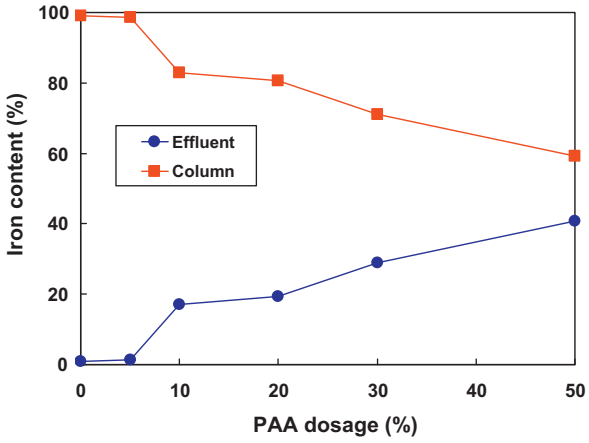

Fig. 8. Iron content distribution between the column and the effluent from the column test with PAA stabilized nZVI at the various PAA dosage.

ratio of iron remained within the column to that in the effluent as a function of the PAA dose for the PAA stabilized nZVI. Even though adding small amounts of PAA (<5%) was not enough to produce sufficient repulsive forces for effective transport nZVI through the sand media, the increase in the PAA dosage (>20%) improved the mobility of the particles. Accordingly, more iron content was determined in the effluent as increasing in the PAA dosage. Nonetheless there was still 57% of iron trapped in the column even at the PAA dosage of 50%. Though the nZVI stabilized with PAA may has lower transport efficiency than that with PV3A, the results shown here imply that a travel-distance-tunable nZVI may be designed to form an iron reactive barrier for the field remediation based upon the use of the PAA as the stabilizer.

4. Conclusions

Because of the large specific surface area and potent reducing power, nZVI has found increasing environmental applications. However, both laboratory and field data show that mobility of nZVI under the natural groundwater flow conditions is very limited. We have examined PV3A and PAA as stabilizers for enhanced transport of nZVI in continuous packed columns. Effects of nZVI stabilization by soy proteins were also tested using batch sedimentation experiments. Because it is an essential for field applications to use high injection concentrations of nZVI, to the best of our knowledge, this study is the first one to investigate nZVI stabilization and transport at relatively high concentrations (10 g/L). Based upon the experimental results, the following conclusions can be drawn:

- PV3A and PAA promote dispersion and improve the transport efficiency of nZVI in the sand column experiments. PV3A has the best performance. PV3A stabilized nZVI readily passes through the sandy column without noteworthy retardation.
- Experiments with PAA stabilized nZVI demonstrate the concentration effect of PAA. Increasing the PAA dosage leads to higher mobility of nZVI; however, there is no additional benefit to the nZVI stability when the PAA dosage is higher than 50%.
- The column experiments show that the PAA stabilized nZVI can transport through the column; however, a retardation effect was observed. At the PAA dose of 50%, approximately 57% of nZVI still remained in the column.
- Soy proteins, which are less expensive, work well at the dosage of 30%. Column tests are still needed in order to better understand the transport behavior of the soy protein stabilized nZVI.

References

[1] C.B. Wang, W.X. Zhang, Synthesizing nanoscale iron particles for rapid and complete dechlorination of TCE and PCBs, Environ. Sci. Technol. 31 (1997) 2154–2156.
[2] W.X. Zhang, Nanoscale iron particles for environmental remediation: an overview, J. Nanopart. Res. 5 (2003) 323–332.
[3] L. Li, M. Fan, R.C. Brown, J. (Hans) Van Leeuwen, J. Wang, W. Wang, Y. Song, P. Zhang, Synthesis, properties, and environmental applications of nanoscale iron-based materials: a review, Crit. Rev. Environ. Sci. Technol. 36 (2006) 405–431.
[4] D.W. Elliott, H.L. Lien, W.X. Zhang, Degradation of lindane by zero-valent iron nanoparticles, J. Environ. Eng. 135 (2009) 317–324.
[5] Z. Xiong, D. Zhao, G. Pan, Rapid and complete destruction of perchlorate in water and ion-exchange brine using stabilized zero-valent iron nanoparticles, Water Res. 41 (2007) 3497–3505.
[6] H.L. Lien, W.X. Zhang, Nanoscale Pd/Fe bimetallic particles: catalytic effects of palladium on hydrodechlorination, Appl. Catal. B: Environ. 77 (2007) 110–116.
[7] H. Song, E.R. Carraway, Reduction of chlorinated ethanes by nanosized zero-valent iron: kinetics, pathways, and effects of reaction conditions, Environ. Sci. Technol. 39 (2005) 6237–6245.
[8] S.R. Kanel, B. Manning, L. Charlet, H. Choi, Removal of arsenic(III) from groundwater by nanoscale zero-valent iron, Environ. Sci. Technol. 39 (2005) 1291–1298.
[9] S.M. Ponder, J.G. Darab, T.E. Mallouk, Remediation of Cr(VI) and Pb(II) aqueous solutions using supported nanoscale zero-valent iron, Environ. Sci. Technol. 34 (2000) 2564–2569.
[10] X.Q. Li, W.X. Zhang, Iron nanoparticles: the core–shell structure and unique properties for Ni(II) sequestration, Langmuir 22 (2006) 4638–4642.
[11] G.V. Lowry, K.M. Johnson, Congener-specific dechlorination of dissolved PCBs by microscale and nanoscale zerovalent iron in a water/methanol solution, Environ. Sci. Technol. 38 (2004) 5208–5216.
[12] C.M. Su, R.W. Puls, Nitrate reduction by zerovalent iron: effects of formate, oxalate, citrate, chloride, sulfate, borate, and phosphate, Environ. Sci. Technol. 38 (2004) 2715–2720.
[13] D.W. Elliott, W.X. Zhang, Field assessment of nanoscale biometallic particles for groundwater treatment, Environ. Sci. Technol. 35 (2001) 4922–4926.
[14] Y.T. Wei, S.C. Wu, C.M. Chou, C.H. Che, S.M. Tsai, H.L. Lien, Influence of nanoscale zero-valent iron on geochemical properties of groundwater and vinyl chloride degradation: a field case study, Water Res. 44 (2010) 131–140.
[15] F. He, D.Y. Zhao, C. Paul, Field assessment of carboxymethyl cellulose stabilized iron nanoparticles for in situ destruction of chlorinated solvents in source zones, Water Res. 44 (2010) 2360–2370.
[16] K.W. Henn, D.W. Waddill, Utilization of nanoscale zero-valent iron for source remediation—a case study, Remediation J. 16 (2006) 57–77.
[17] J. Quinn, C. Geiger, C. Clausen, K. Brooks, C. Coon, S. O'Hara, T. Krug, D. Major, W.S. Yoon, A. Gavaskar, T. Holdsworth, Field demonstration of DNAPL dehalogenation using emulsified zero-valent iron, Environ. Sci. Technol. 39 (2005) 1309–1318.
[18] Y.P. Sun, X.Q. Li, J.S. Cao, W.X. Zhang, H.P. Wang, Characterization of zero-valent iron nanoparticles, Adv. Colloid Interface Sci. 120 (2006) 47–56.
[19] Y.P. Sun, X.Q. Li, W.X. Zhang, H.P. Wang, A method for the preparation of stable dispersion of zero-valent iron nanoparticles, Colloids Surf. A 308 (2007) 60–66.
[20] T. Phenrat, N. Saleh, K. Sirk, R.D. Tilton, G.V. Lowry, Aggregation and sedimentation of aqueous nanoscale zerovalent iron dispersions, Environ. Sci. Technol. 41 (2007) 284–290.
[21] W. Stumm, J.J. Morgan, Aquatic Chemistry: Chemical Equilibria and Rates in Natural Waters, third ed., John Wiley & Sons, Inc., New York, 1996.
[22] B. Schrick, B.W. Hydutsky, J.L. Blough, T.E. Mallouk, Delivery vehicles for zerovalent metal nanoparticles in soil and groundwater, Chem. Mater. 16 (2004) 2187–2193.
[23] F. He, D.Y. Zhao, Preparation and characterization of a new class of starch-stabilized bimetallic nanoparticles for degradation of chlorinated hydrocarbons in water, Environ. Sci. Technol. 39 (2005) 3314–3320.
[24] T. Phenrat, N. Saleh, K. Sirk, H. Kim, R.D. Tilton, G.V. Lowry, Stabilization of aqueous nanoscale zerovalent iron dispersions by anionic polyelectrolytes: adsorbed anionic polyelectrolyte layer properties and their effect on aggregation and sedimentation, J. Nanopart. Res. 10 (2008) 795–814.
[25] A. Tiraferri, K.L. Chen, R. Sethi, M. Elimelech, Reduced aggregation and sedimentation of zero-valent iron nanoparticles in the presence of guar gum, J. Colloid Interface Sci. 324 (2008) 71–79.
[26] H.J. Kim, T. Phenrat, R.D. Tilton, G.V. Lowry, Fe^0 nanoparticles remain mobile in porous media after aging due to slow desorption of polymeric surface modifiers, Environ. Sci. Technol. 43 (2009) 3824–3830.
[27] N. Saleh, K. Sirk, Y. Liu, T. Phenrat, B. Dufour, K. Matyjaszewski, R.D. Tilton, G.V. Lowry, Surface modifications enhance nanoiron transport and NAPL targeting in saturated porous media, Environ. Eng. Sci. 24 (2007) 45–57.
[28] N. Saleh, H.J. Kim, T. Phenrat, K. Matyjaszewski, R.D. Tilton, G.V. Lowry, Ionic strength and composition affect the mobility of surface-modified Fe^0 nanoparticles in water-saturated sand columns, Environ. Sci. Technol. 42 (2008) 3349–3355.
[29] D.H. Everett, Basic Principles of Colloid Science, Royal Society of Chemistry, London, 1989.
[30] X.Q. Li, D.W. Elliott, W.X. Zhang, Zero-valent iron nanoparticles for abatement of environmental pollutants: materials and engineering aspects, Crit. Rev. Solid State Mater. Sci. 31 (2006) 111–122.
[31] I.D. Morrison, S. Ross, Colloidal Dispersions: Suspensions, Emulsions and Foams, Wiley–Interscience, New York, 2002.
[32] G.C.C. Yang, H.C. Tu, C.H. Hung, Stability of nanoiron slurries and their transport in the subsurface environment, Sep. Purif. Technol. 58 (2007) 166–172.
[33] S.R. Kanel, D. Nepal, B. Manning, H. Choi, Transport of surface-modified iron nanoparticle in porous media and application to arsenic(III) remediation, J. Nanopart. Res. 9 (2007) 725–735.
[34] T. Phenrat, A. Cihan, H.J. Kim, M. Mital, T. Illangasekare, G.V. Lowry, Transport and deposition of polymer-modified Fe^0 nanoparticles in 2-D heterogeneous porous media: effects of particle concentration, Fe^0 content, and coatings, Environ. Sci. Technol. 44 (2010) 9086–9093.
[35] T Raychoudhury, G. Naja, S. Ghoshal, Assessment of transport of two polyelectrolyte-stabilized zero-valent iron nanoparticles in porous media, J. Contam. Hydrol. 118 (2010) 143–151.
[36] L.A. Harris, J.D. Goff, A.Y. Carmichael, J.S. Riffle, J.J. Harburn, T.G. St Pierre, M. Saunders, Magnetite nanoparticle dispersions stabilized with triblock copolymers, Chem. Mater. 15 (2003) 1367–1377.
[37] N.Q. Wu, L. Fu, M. Su, M. Aslam, K.C. Wong, V.P. Dravid, Interaction of fatty acid monolayers with cobalt nanoparticles, Nano Lett. 4 (2004) 383–386.
[38] R.P. Wool, X.S. Sun, Chapter 9: Thermal and Mechanical Properties of Soy Proteins in Bio-Based Polymers and Composites, Academic Press, 2005, pp. 292–293.

[39] P.B. Bedient, H.S. Rifal, C.J. Newell, Ground Water Contamination: Transport and Remediation, Prentice-Hall, 1999.
[40] N. Tufenkji, M. Elimelech, Correlation equation for predicting single-collector efficiency in physicochemical filtration in saturated porous media, Environ. Sci. Technol. 38 (2004) 529–536.
[41] S.R. Kanel, R.R. Goswsmi, T.P. Clement, M.O. Barnett, D. Zhao, Two dimensional transport characteristics of surface stabilized zero-valent iron nanoparticles in porous media, Environ. Sci. Technol. 42 (2008) 896–900.
[42] T.K. Sen, K.C. Khilar, Review on subsurface colloids and colloid-associated contaminant transport in saturated porous media, Adv. Colloid Interface Sci. 119 (2006) 71–96.
[43] H.L. Lien, Y.S. Jhuo, L.H. Chen, Effect of heavy metals on dechlorination of carbon tetrachloride by iron nanoparticles, Environ. Eng. Sci. 24 (2007) 21–30.
[44] Y.H. Lin, H.H. Tseng, M.Y. Wey, M.D. Lin, Characteristics of two types of stabilized nano zero-valent iron and transport in porous media, Sci. Total Environ. 408 (2010) 2260–2267.